ISBN: 978-3-95450-211-0 doi:10.18429/JACoW-SRF2019-THP103

RECONSTRUCTION OF THE LONGITUDINAL PHASE SPACE FOR THE SUPERCONDUCTING CW HELIAC

S. Lauber*[1,2,4], K. Aulenbacher [1,2,4], W. Barth[1,2], C. Burandt[1,2], F. Dziuba[1,2,4], P. Forck[2], V. Gettmann[1,2], M. Heilmann[2], T. Kürzeder[1,2], J. List[1,2,4], M. Miski-Oglu[1,2], H. Podlech[3], M. Schwarz[3], T. Sieber[2], S. Yaramyshev[2]
[1] Helmholtz Institute Mainz, Mainz, Germany
[2]GSI Helmholtzzentrum für Schwerionenforschung, Darmstadt, Germany
[3]Goethe-University, Frankfurt, Germany
[4]Johannes Gutenberg-University, Mainz, Germany

Abstract

The superconducting (SC) heavy ion HElmholtz LInear ACcelerator (HELIAC) is under development at GSI in Darmstadt in cooperation with Helmholtz Institute Mainz (HIM) and Goethe-University Frankfurt (GUF). A novel design is used for the accelerating cavities, namely SC continuous wave (CW) multigap Crossbar H-Mode cavities. For this a dedicated beam dynamics layout - the EQUidistant mUltigap Structure (EQUUS) - has been carried out a couple of years ago and is under further development. In December 2018 the GSI High Charge State Injector (HLI) delivered heavy ion beam to the already commissioned first of series superconducting RF cavity. Proper 6D-matching to the CH cavity demands sufficient beam characterisation. Slit-grid emittance measurements provided for the transverse phase space determination. By measuring the longitudinal projection of the bunch with a Feschenko Monitor (Beam Shape Monitor), the bunch profile was obtained. With a dedicated algorithm, the full longitudinal phase space at the HLI-exit could be reconstructed from a set of BSM measurements. The basic reconstruction method, all relevant BSM measurements and the resulting phase space reconstruction will be presented.

INTRODUCTION

For the Super Heavy Elements (SHE) research collision experiments with medium to heavy ions on heavy targets are used to cause fusion-evaporation reactions. Extremely small cross-sections make a long beam time crucial for these type of experiments [1,2]. Whilst the GSI Universal Linear Accelerator (UNILAC) [3–7] is upgraded as an exclusive injector for the Facility for Antiproton and Ion Research (FAIR) [6,7], a new superconducting continuous wave (CW) heavy ion linear accelerator (Linac) is built at GSI to keep the SHE research competitive. This project is carried out by the GSI and the HIM [8,9] under key support of the GUF [10,11] and in collaboration with the Moscow Engineering Physics Institute (MEPhI) and the Moscow Institute for Theoretical and Experimental Physics (KI-ITEP) [12,13]. For different modern facilities worldwide, the operation of CW Linacs is crucial, as for the Spallation Neutron Source (SNS) in the U.S. [14], or medium energy applications in isotope generation, material science and boron-neutron capture therapy [15]. Therefore, the progress in SRF in particular for superconducting multi gap cavities [16] and its operation is a decisive contribution to global accelerator development.

* s.lauber@gsi.de

Helmholtz Linear Accelerator

A new warm injector will provide for a 1.4 MeV/u CW heavy ion beam to the main superconducting HELIAC [17]. It comprises a radio frequency quadrupole (RFQ) and an interdigital H-Mode cavity (IH) together with two rebuncher cavities. Four cryomodules with compact SC CH cavities, SC solenoids and SC rebunchers [11] form the SC HELIAC section. Key features of the accelerator are a variable output energy (see Table 1) and the capability to provide for CW operation, while keeping the momentum spread low.

Table 1: HELIAC Design Specifications [17]

	Value
Mass/charge	≤ 6
Frequency	216.816 MHz
Maximum beam current	1 mA
Injection energy	1.4 MeV/u
Variable output energy	3.5 MeV/u to 7.3 MeV/u
Output energy spread	±3 keV/u

The HELIAC stays in line with diverse ambitious Linac projects at GSI, namely the FAIR proton Linac [18], the UNILAC proton beam delivery [19–21], the linear heavy ion decelerator HITRAP (Heavy Ion TRAP) [22] and the LIGHT (Laser Ion Generation, Handling and Transport) facility for laser acceleration of protons and heavy ions [23].

Demonstrator Environment

The novel CH design was tested and validated by two measurement campaigns in 2017 and 2018, where CH0 as a first of series was tested extensively [17, 24, 25]. Beam from HLI has been delivered to CH0 (installed in a test cryomodule) [26]. The IH-DTL as main part of the HLI is designed with the KOmbinierte NUll Grad Struktur (KONUS) beam dynamics concept [27, 28], which introduces a nonlinear transformation to the bunch shape in the longitudinal phase plane. This arises from using different RF phases in

ISBN: 978-3-95450-211-0 doi:10.18429/JACoW-SRF2019-THP103

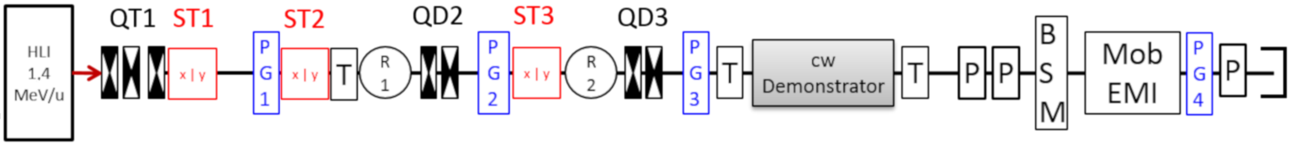

Figure 1: Beam line 2018. QT: Quadrupole Triplet, QD: Quadrupole Duplet, R: Rebuncher, X|Y: Beam Steerer, G: SEM-Grid, T: Beam Current Transformer, P: Phase Probe, BSM: Bunch Shape Monitor, EMI=Emittance Meter [17].

each acceleration gap instead of applying −30 degree constantly. For longitudinal and transversal matching of the beam to the demonstrator cryomodule, two rebunchers, two quadrupole duplets and a quadrupole triplet are mounted, as well as three beam steerers for alignment (see Fig. 1). Phase probe sensors were used to determine the beam energy by Time Of Flight (ToF) measurements. The beam profile and position could be measured with Secondary Electron EMission (SEM) grids. For longitudinal bunch shape measurements [29] a Feschenko-Monitor [30] was used.

Principle of Tomographic Reconstruction

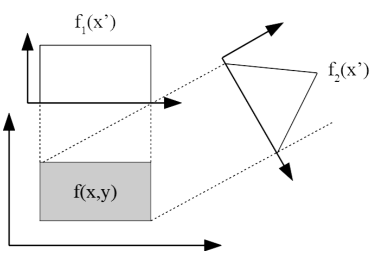

Figure 2: Example of reconstruction setup for a linear transformation between image and histogram. The observed histograms $f_i(x')$ constrain the shape of the reconstructed object [31].

The distribution $f(x, y)$ (see Fig. 2) has to be recalculated from a set of projections $f_i(x')$. The tomographic reconstruction method also appears in medical diagnostics, where it is used for body imaging. A wide range of reconstruction algorithms already exists for clinical purpose, but they are commonly formulated using linear mappings between $f(x, y)$ and $f_i(x')$ (see Fig. 2), or explicitly base on rotation transformations. For accelerator applications, it is generally not possible to rotate the beam. Optical elements in the beam line are used to alter the bunch shape, which in most cases is characterized by shearing. When the bunch transormation can be expressed in this way, it is possible to preprocess the data into a sinogram to be used as input for common reconstruction algorithms. In some cases, the bunch transfer is not linear, therefore it is not useful to use sinograms. Suitable algorithms have to be adjusted to this scenarios. The Algebraic Reconstruction Technique (ART) [32] and the Maximum Entropy Tomography Reconstruction (MENT) [33] already have been used for longitudinal phase space reconstruction [33,34]. A different approach has been investigated for the HELIAC. Instead of using ART or MENT, a Non Negative Least Squares (NNLS) [35] is used to solve the reconstruction problem the longitudinal phase plane.

METHODS

To infer the unknown bunch shape in the longitudinal phase plane, different projections must be obtained. The two rebunchers were used to provide diverse bunch shapes at the Bunch Shape Monitor (BSM) therefore.

Bunch Shape Monitor

The Feschenko Monitor mounted behind the Demonstrator was used for the series of measurements, which were used as input for the reconstruction algorithm. The device provides for measurements of the longitudinal bunch shape of heavy ions and offers a high signal to noise ratio and a phase resolution of up to 1 degree with respect to 108.408 MHz. A detailed description of the Feschenko Monitor is given in [30].

Reconstruction

For the reconstruction, the relation from the input coordinates at the beginning of the beam line (i.e. exit of the HLI) to the coordinates at the Feschenko Monitor must be known. The beamline could be described by using the particle tracking code DYNAMION [36], which allows to monitor individual particles along their trajectory. Disposing a grid as input distribution and tracking it through the beamline, the mapping from HLI to BSM $\vec{f}_i(\vec{x}_{\text{in}})$ could be described for each buncher setting i, as well as the projection to the longitudinal spatial axis $A_i(\phi, \vec{X}_{\text{in}})$ for a set of input coordinates $\vec{X}_{\text{in}}$. For a given particle output phase ϕ, a set of input coordinates $\vec{x}_{\text{in},i}$ exists: $\vec{x}_{\text{in},i}(\phi)$ is ambiguous. In order to determine the boundaries, which are used for NNLS reconstruction, the back tracking function $\vec{x}_{\text{in},i}(\phi)$ can be used to select the area of interest for reconstruction. All phases ϕ, where the signal is below a certain threshold, are selected and tracked back for each histogram. Two areas can be distinguished: areas with signal and areas without signal. By summing up these areas of every histogram, an image can be produced, describing the amount of histograms holding signal/no signal: $N_i(\vec{x}_{\text{in}}) = |\{\phi_i(\vec{x}_{\text{in}})|A(\phi_i(\vec{x}_{in})) \neq 0\}|$.

Furthermore, the mapping $A_i(\phi, \vec{X}_{\text{in}})$ can be expressed in terms of a matrix multiplication $\vec{A}_i = B_i \cdot \vec{X}$ for discrete values $\vec{f}_i(\phi, p)$, which are assembled into X. With this discretization, also nonlinear mappings can be expressed in terms of B_i, which is useful to determine the input distribution $\vec{X}$ with given measurements $\vec{A}_i$. Therefore, all mappings

ISBN: 978-3-95450-211-0 doi:10.18429/JACoW-SRF2019-THP103

and all measurements can be stacked up into one equation $\vec{A} = B \cdot \vec{X}$. Also, a negative particle count for the input distribution is not considered. Therefore the task can be expressed as Non Negative Least Squares problem:

$$\text{argmin}_{\vec{X}} ||B\vec{X} - \vec{A}||_2 \text{ subject to } \vec{X} \geq 0 \tag{1}$$

The mapping B of the artificial input distribution $\vec{X}$ to all measured histograms $\vec{A}$ should show minimal difference.

RESULTS

Measurements

All elements in the matching line, excluding the rebunchers, were set to a state of minimal beam loss for a wide range of rebuncher focusing strengths. 100 BSM-measurements have been conducted with Ar^{9+} beam from the HLI. Combinations of different rebuncher voltages ($R1$,$R2$) were applied, providing for a detailed transition from defocusing to overfocusing. Exemplary measurements are presented in Fig. 3. As one can see from the histograms, the beam shape

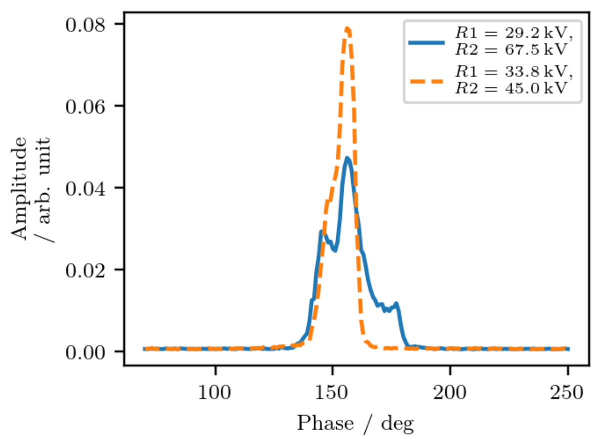

Figure 3: Bunch shape samples for two different rebuncher settings measured with the BSM (108 MHz).

is non-symmetrical due to the KONUS beam dynamics of the HLI-IH-DTL. This makes the use of an advanced reconstruction technique necessary, which considers a non elliptic shape.

Conservative preprocessing was applied to the measurement data. 6 % of the amplitudes were cut to remove unwanted background. The histograms were recentered to their center of mass. In good accordance to the measurements the transmission was assumed to be 100 %.

The measurements of the BSM are presented, so that the head of the bunch is displayed on the right side, the tail on the left (Phase $\propto +z$). In the following, the phase planes are displayed to the same convention.

Reconstruction

As described in the previous section, the back projection of the histograms can be used to determine the area of the bunch in the longitudinal phase space. These limits can be used as constraints of the NNLS solver. This two step procedure enhances the analysis performance and increases the reliability by using two methods. Resulting from the back

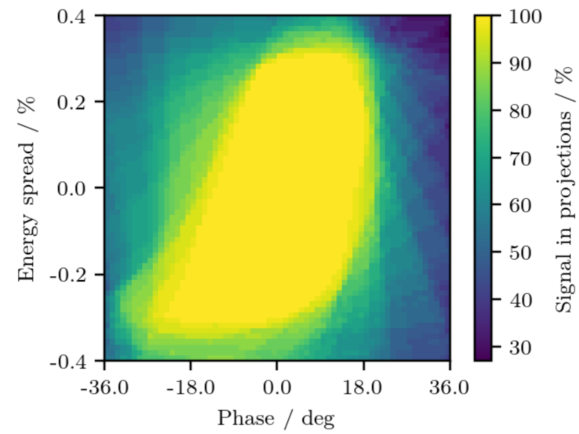

Figure 4: By back projecting the histograms to the input plane, areas can be marked where signal is absent and vice versa.

projection properties, a signal of 0 % can not be achieved by overlapping projections from different "directions". For the yellow area (100 % in Fig. 4) the RMS-emittance could be evaluated for $\epsilon_{\text{RMS}} = 18$ keV/u deg . This emittance is in good agreement with the former simulations of the HLI, which yielded an RMS emittance of 13.5 keV/u deg [37]. The reconstructed emittance is slightly increased, as the shape reconstruction does not distinguish between low and high signal strengths. By using the limits shown in Fig. 4, the NNLS solver was applied to reconstruct the exact bunch shape and density distribution with the derived boundary values. The NNLS solver reveals a more complicated shape (see Fig. 5).

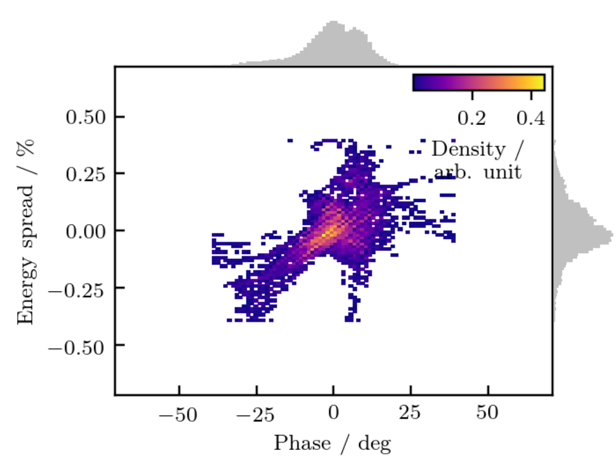

Figure 5: Reconstructed phase space with the NNLS solver (108 MHz).

The full emittance is $\epsilon_{\text{RMS}} = 27.3$ keV/u deg . In the cen-

ISBN: 978-3-95450-211-0 doi:10.18429/JACoW-SRF2019-THP103

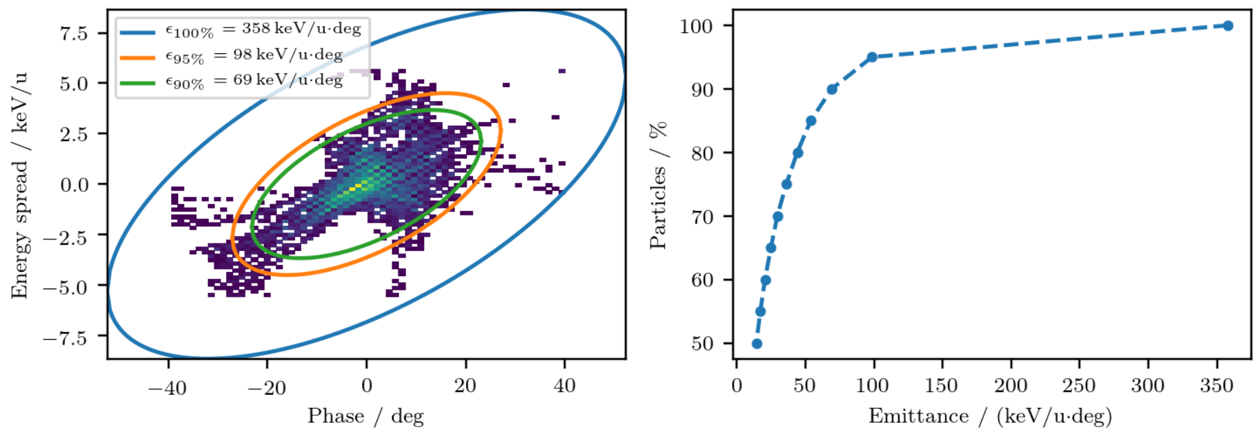

Figure 6: Brilliance analysis of the reconstructed distribution. Samples of the fitted ellipses around a fraction of the density distribution (left) and relation of the emittance on the fraction of particles (right).

ter of the distribution, a remarkably small spot with high intensity can be recognized. The analysis of the reconstructed emittance is presented in Fig. 6. Selected ellipses surrounding a fraction of the particles are displayed. The 100 % emittance of the bunch is dominated by marginal particles (5 % of the particle distribution), while most of the particles are concentrated in the center. The reconstructed emittance coincide with the assumptions for the design of the accelerator. Recently, the BSM was mounted and commissioned at a different position (at the exit of the injector HLI) and a dedicated measurement campaign is foreseen to compare new measurements to the reconstruction result.

CONCLUSION & OUTLOOK

A sufficient amount of data has been collected to perform the reconstruction of the longitudinal phase space. The longitudinal bunch shape and its density distribution could be reconstructed with the NNLS algorithm using results of the beam dynamics code DYNAMION. From now on the matching of the beam to the Demonstrator and to the HELIAC can be investigated with a higher level of detail to further improve the performance of the system. It is foreseen to cross check the reconstruction results by comparing the reconstructed and measured longitudinal bunch projection at the exit of the HLI. For the design beam current of 1 mA, additional considerations of space charge must be taken into account for future measurements.

REFERENCES

[1] M. Block *et al.*, "Direct mass measurements above uranium bridge the gap to the island of stability", *Nature*, vol. 463, pp. 785–788, Feb. 2010. doi:10.1038/nature08774

[2] J. Khuyagbaatar *et al.*, "^{48}Ca + ^{249}Bk Fusion reaction leading to element Z=117: long-lived α-decaying ^{270}Db and discovery of ^{266}Lr", *Phys. Rev. Lett.*, vol. 112, no. 17, p. 172501, May 2014. doi:10.1103/PhysRevLett.112.172501

[3] W. Barth *et al.*, "U^{28+} intensity record applying a H_2 gas stripper cell", *Phys. Rev. ST Accel. Beams*, vol 18, p. 040101, Apr. 2015. doi:10.1103/PhysRevSTAB.18.040101

[4] A. Adonin *et al.*, "Beam brilliance investigation of high current ion beams at GSI heavy ion accelerator facility", *Rev. Sci. Instrum.*, vol. 85, p. 02A727, Apr. 2014. doi:10.1063/1.4833931

[5] S. Yaramyshev *et al.*, "Virtual charge state separator as an advanced tool coupling measurements and simulations", *Phys. Rev. ST Accel. Beams*, vol. 18, p. 050103, Sept. 2015. doi:10.1103/PhysRevSTAB.18.050103

[6] W. Barth *et al.*, "High brilliance uranium beams for the GSI FAIR", *Phys. Rev. ST Accel. Beams*, vol. 20, p. 050101, May 2017. doi:10.1103/PhysRevAccelBeams.20.050101

[7] W. Barth *et al.*, "Upgrade program of the high current heavy ion UNILAC as an injector for FAIR", *Nucl. Instr. Meth. Phys. Res. Sect. A*, vol. 577, no. 1-2, pp. 211—214, Jul. 2007. doi:10.1016/j.nima.2007.02.054

[8] W. Barth *et al.*, "Superconducting CH-Cavity heavy ion beam testing at GSI", *J. Phys. Conf. Ser.*, vol. 1067, no. 5, p. 052007, Sept. 2018. doi:10.1088/1742-6596/1067/5/052007

[9] F. D. Dziuba *et al.*, "First Cold Tests of the Superconducting cw Demonstrator at GSI", in *Proc. RuPAC'16*, Saint Petersburg, Russia, Nov. 2016, pp. 84–86. doi:10.18429/JACoW-RUPAC2016-WECBMH01

[10] H. Podlech *et al.*, "Superconducting CH structure", *Phys. Rev. ST Accel. Beams*, vol. 10, no. 8, p. 080101, Aug. 2007. 10.1103/PhysRevSTAB.10.080101

[11] M. Schwarz *et al.*, "Beam dynamics simulations for the new superconducting CW heavy ion Linac at GSI", *J. Phys.: Conf. Ser.*, vol. 1067, 052006, Oct. 2018. doi:10.1088/1742-6596/1067/5/052006

[12] M. Gusarova *et al.*, "Design of the two-gap superconducting re-buncher", *J. Phys.: Conf. Ser.*, vol. 1067, p. 082005, Oct. 2018. doi:10.1088/1742-6596/1067/8/082005

[13] K. Taletskiy *et al.*, "Comparative study of low beta multi-gap superconducting bunchers", *J. Phys.: Conf. Ser.*, vol. 1067, p. 082006, Oct. 2018. doi:10.1088/1742-6596/1067/8/082006

[14] S.M. Polozov and A.D. Fertman, "High-energy proton beam accelerators for subcritical nuclear reactors", *At. Energ.*, vol. 113, no. 3, pp. 192–200, Jan. 2013. doi:10.1007/s10512-012-9616-4

[15] Zhi-Jun Wang *et al.*, "Beam commissioning for a superconducting proton Linac", *Phys. Rev. Accel. Beams*, vol. 19, p. 120101, Dec. 2016. doi:10.1103/PhysRevAccelBeams.19.120101

[16] R. Laxdal *et al.*, "Recent progress in the superconducting RF Program at TRIUMF/ISAC", *Physica C: Superconductivity* vol. 441, no. 1-2, pp. 13, Jul. 2006. doi:10.1016/j.physc.2006.03.096

[17] W. Barth *et al.*, "First heavy ion beam tests with a superconducting multigap CH cavity", *Phy. Rev. Accel. Beams*, vol. 21, no. 2, p. 020102, Feb. 2018. doi:10.1103/PhysRevAccelBeams.21.020102

[18] U. Ratzinger *et al.*, "The 70 MeV p-injector design for FAIR", *AIP Conf. Proc.*, Vol. 773, pp 249-253, 2005. doi:10.1063/1.1949539

[19] W. Barth *et al.*, "Heavy ion Linac as a high current proton beam injector", *Phys. Rev. ST Accel. Beams*, vol. 18,p. 050102, Sep. 2015. doi:10.1103/PhysRevSTAB.18.050102

[20] A. Adonin *et al.*, "Production of high current proton beams using complex H-rich molecules at GSI", *Rev. Sci. Instrum.*, vol. 87, 02B709, 2016. doi:10.1063/1.4934620

[21] P. Forck, "Minimal Invasive Beam Profile Monitors for High Intense Hadron Beams", in *Proc. IPAC'10*, Kyoto, Japan, May 2010, paper TUZMH01, pp. 1261–1265.

[22] F. Herfurth *et al.*, "The HITRAP facility for slow highly charged ions", *Physica Scripta* vol. 2015, no. T166, 014065, Nov. 2015. doi:10.1088/0031-8949/2015/t166/014065

[23] S. Busold *et al.*, "Shaping laser accelerated ions for future applications - The LIGHT collaboration", *Nucl. Instrum. Meth. Phys. Res. Sect. A*, vol. 740, pp. 94-98, Mar. 2014. doi:10.1016/j.nima.2013.10.025

[24] S. Yaramyshev *et al.*, "Advanced approach for beam matching along the multi-cavity SC CW Linac at GSI", *J. Phys. Conf. Ser.*, vol. 1067, p. 052005, Sep. 2018. doi:10.1088/1742-6596/1067/5/052005

[25] S. Minaev *et al.*, "Superconducting, energy variable heavy ion Linac with constant β, multicell cavities of CH-type", *Phys. Rev. ST Accel. Beams*, vol. 12, p. 120101, Dec. 2009. doi:10.1103/PhysRevSTAB.12.120101

[26] P. Gerhard *et al.*, "Commissioning of a New CW Radio Frequency Quadrupole at GSI", in *Proc. IPAC'10*, Kyoto, Japan, May 2010, paper MOPD028, pp. 741–743.

[27] R. Tiede, G. Clemente, H. Podlech, U. Ratzinger, and C. Zhang, "KONUS Beam Dynamics Designs Using H-Mode Cavities", in *Proc. HB'08*, Nashville, TN, USA, Aug. 2008, paper WGB11, pp. 223–230.

[28] R. Tiede, G. Clemente, S. Minaev, H. Podlech, U. Ratzinger, and A. C. Sauer, "LORASR Code Development", in *Proc. EPAC'06*, Edinburgh, UK, Jun. 2006, paper WEPCH118, pp. 2194–2196.

[29] T. Sieber *et al.*, "Bunch Shape Measurements at the GSI CW-Linac Prototype", in *Proc. IPAC'18*, Vancouver, Canada, Apr.-May 2018, pp. 2091–2094. doi:10.18429/JACoW-IPAC2018-WEPAK006

[30] A. V. Feschenko, "Methods and Instrumentation for Bunch Shape Measurements (Invited)", in *Proc. PAC'01*, Chicago, IL, USA, Jun. 2001, paper ROAB002, pp. 517-521.

[31] S. Lauber *et al.*, "Reconstruction of the Longitudinal Phase Portrait for the SC CW Heavy Ion HELIAC at GSI", in *Proc. IPAC'19*, Melbourne, Australia, May 2019, paper MOPTS024, pp. 898-901.

[32] R. Gordon, R. Bender, and G. T. Herman, "Algebraic Reconstruction Techniques (ART) for three-dimensional electron microscopy and X-ray photography", *J. Theor. Biol.*, vol. 29, no. 3, pp. 471-476, Dec. 1970. doi:10.1016/0022-5193(70)90109-8

[33] K. M. Hock *et al.*, "Beam tomography research at Daresbury Laboratory", *Nucl. Instr. Meth. Phys. Res. Sect. A*, vol. 753, no. 1, pp. 38-55, Jul. 2014. doi:10.1016/j.nima.2014.03.050

[34] D. Malyutin *et al.*, "Longitudinal phase space tomography using a booster cavity at PITZ", *Nucl. Instr. Meth. Phys. Res. Sect. A*, vol. 871, no. 1, Nov. 2017, pp. 105-112. doi:10.1016/j.nima.2017.07.043

[35] C. L. Lawson and R. J. Hanson, *Solving least squares problems*. Philadelphia, PA, USA: Society for Industrial and Applied Mathematics, 1987.

[36] S. Yaramyshev *et al.*, "Development of the versatile multiparticle code DYNAMION", *Nucl. Instrum. Meth. Phys. Res. Sect. A*, vol. 558, no. 1, p. 90-95, Mar. 2006. doi:10.1016/j.nima.2005.11.018

[37] U. Ratzinger, "Effiziente Hochfrequenz-Linearbeschleuniger für leichte und schwere Ionen", Habilitation, Phys. Dept., Goethe-University, Frankfurt am Main, Germany, 1998.